

# SPOT: Single-Shot Positioning via Trainable Near-Field Rainbow Beamforming

Yeyue Cai, Jianhua Mo, and Meixia Tao

**Abstract**—Phase-time arrays, which integrate phase shifters (PSs) and true-time delays (TTDs), have emerged as a cost-effective architecture for generating frequency-dependent rainbow beams in wideband sensing and localization. This paper proposes an end-to-end deep learning-based scheme that simultaneously designs the rainbow beams and estimates user positions. Treating the PS and TTD coefficients as trainable variables allows the network to synthesize task-oriented beams that maximize localization accuracy. A lightweight fully connected module then recovers the user’s angle-range coordinates from its feedback of the maximum quantized received power and its corresponding subcarrier index after a single downlink transmission. Compared with existing analytical and learning-based schemes, the proposed method reduces overhead by an order of magnitude and delivers consistently lower two-dimensional positioning error.

**Index Terms**—frequency-dependent beamforming, true-time delay, deep learning, localization.

## I. INTRODUCTION

Integrated sensing and communication (ISAC) combines radar and communication functionalities by sharing hardware and spectral resources, making it a key technology for 5G-Advanced and 6G networks [1]. A key advantage of ISAC is its ability to repurpose communication waveforms, like orthogonal frequency-division multiplexing (OFDM), for user positioning, enabling dynamic beam steering in subsequent transmissions.

In wideband systems, phase-time arrays (PTAs), integrating phase shifters (PSs) and true-time-delays (TTDs), have become a promising architecture for cost-effective and energy-efficient localization [2]–[5]. PTAs synthesize a controllable “rainbow beam” by simultaneously directing different OFDM subcarriers towards distinct spatial directions. This unique feature facilitates rapid scanning and training across broad angular sectors and distance ranges. In contrast, conventional phased arrays generate only a single directional beam per time slot, necessitating sequential beam sweeping spanning multiple time slots. Consequently, PTAs significantly reduce beamforming latency and system overhead in wideband ISAC applications, attracting considerable research interest.

One of the primary applications of PTAs in ISAC systems is user positioning [6]–[9]. Within this framework, the base station (BS) transmits rainbow-like pilot beams covering the entire service area and subsequently estimates user locations based on feedback from the users. In far-field scenarios,

rainbow-beam training schemes have been proposed to recover user angles with reduced overhead [6]. Here, the BS estimates each user’s direction by mapping the reported subcarrier frequency to its corresponding steering angle. In near-field environments, where the spherical wavefront becomes significant, rainbow beams are generated independently in the angular and distance domains to estimate direction and range sequentially [7]. Convolutional neural networks are then employed to refine these initial estimates using the received signal [8]. A distance-dependent rainbow-beam method further reduces overhead by enabling joint angle and distance estimation within a beam [9]. In contrast to the aforementioned cooperative approaches, a deep learning-based uplink near-field positioning method, called RaiNet, was proposed in [10]. The BS observes the full-band amplitude response vector, and a convolutional backbone regresses the 2D position in a single shot.

As discussed above, existing PTA-based sensing methods in wideband systems predominantly rely on rainbow beams that map frequency to either angle or range [6]–[8]. However, range estimation via frequency–distance mapping is effective primarily in the near-field where the beam can be focused on a specific point. Moreover, these schemes often suffer from high feedback overhead. For instance, studies [6], [7] typically require at least two rounds of downlink beam transmissions and subsequent user feedback to recover both angle and range. The approach presented in [8] further exacerbates this overhead by requiring users to transmit their complete received signal in each feedback instance. The method in [9] can scan the range and angle simultaneously, but multiple beams are needed to cover the whole angle-range space and avoid coverage hole. Moreover, this rainbow-beam design typically covers a wide sector of  $-90^\circ$  to  $90^\circ$ , which is broader than the actual user distribution range (e.g.,  $-60^\circ$  to  $60^\circ$ ), leading to unnecessary beam coverage and resource waste.

To overcome these limitations, we propose a deep learning-based localization scheme capable of recovering both angle and range with only a single downlink beamforming transmission and one-shot user feedback message, referred to as Single-shot POsitioning with Trainable near-field rainbow beamforming (SPOT). In the SPOT scheme, each user identifies the OFDM subcarrier with the maximum received power and reports solely the quantized maximum received power and the index of the corresponding subcarrier. The BS then infers the user’s range and angle based on the user feedback. Furthermore, to ensure robust performance across both near- and far-field regions, we

The authors are with the Cooperative Medianet Innovation Center (CMIC), Shanghai Jiao Tong University, China (Email: {cayeyue, mjh, mx-tao}@sjtu.edu.cn). Corresponding authors: *Meixia Tao* and *Jianhua Mo*.

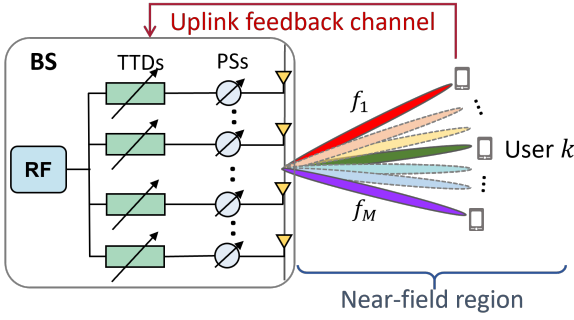


Fig. 1: System model.

deviate from prior works that determine PS and TTDs values heuristically. Instead, we treat the settings of PS and TTDs as learnable network parameters. This joint optimization process yields rainbow beams that are inherently optimized for accurate position estimation across all propagation regimes.

## II. SYSTEM MODEL

We consider an OFDM wideband ISAC system, where the BS is equipped with a single radio frequency (RF) chain connected to a uniform linear array (ULA) consisting of  $N$  elements. As shown in Fig. 1, we employ a PTA architecture to generate rainbow-like beams for radar sensing of  $K$  users. The line-of-sight (LoS) channel model is assumed for all the  $K$  users. In the PTA architecture, the single RF chain is connected to all  $N$  transmit antennas via  $N$  PSs and  $N$  TTDs. The system utilizes  $M$  orthogonal subcarriers. Let  $B$  denote the system bandwidth and  $f_c$  the central carrier frequency. Accordingly, subcarrier  $m$  has a center frequency of  $f_m = f_c + \frac{(2m-1-M)}{2} f_{scs}$ ,  $\forall m \in \{1, 2, \dots, M\}$ , where subcarrier spacing  $f_{scs} = \frac{B}{M}$ .

The position of user  $k$  relative to the center of the ULA at the BS is characterized by the angle  $\theta_k$  and distance  $r_k$ . The coordinates of user  $k$  and the  $n$ -th element of the ULA are denoted by  $\mathbf{u}_k = [r_k \cos \theta_k, r_k \sin \theta_k]^T$  and  $\mathbf{c}_n = [x_n d, 0]^T$ ,  $\forall n \in \{1, 2, \dots, N\}$ , where  $x_n = n - \frac{N+1}{2}$  and antenna spacing  $d = \frac{c}{2f_c}$ . In the near-field region, the propagation distance from the  $n$ -th antenna element to user  $k$  is approximated following the spherical wave model as

$$r_{k,n} = \|\mathbf{u}_k - \mathbf{c}_n\| \approx r_k - x_n d \cos \theta_k + \frac{x_n^2 d^2 \sin^2 \theta_k}{2r_k}. \quad (1)$$

The LoS channel for subcarrier  $m$  of user  $k$  is modeled as

$$\mathbf{h}_{k,m} = \beta_k e^{j \frac{2\pi f_m r_k}{c}} \mathbf{a}_{m,k}, \quad (2)$$

where  $\beta_k = \frac{c}{4\pi f_m r_k}$  denotes the path loss, and  $\mathbf{a}_{m,k}$  is the array response vector, which is given by

$$\mathbf{a}_{m,k} = \left[ e^{-j \frac{2\pi f_m}{c} (r_{k,1} - r_k)}, \dots, e^{-j \frac{2\pi f_m}{c} (r_{k,N} - r_k)} \right]^T. \quad (3)$$

The received signal of user  $k$  on subcarrier  $m$  is

$$y_{k,m} = \mathbf{h}_{k,m}^H e^{j(\Phi - 2\pi f_m \mathbf{T})} s_m + n_{k,m}, \quad (4)$$

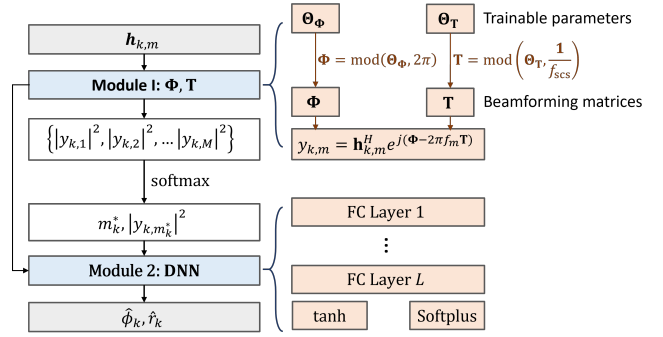


Fig. 2: System architecture of the proposed SPOT scheme.

where  $s_m$  is the transmitted signal at the  $m$ -th subcarrier and  $n_{k,m}$  denotes the additive noise. Vectors  $\Phi \in \mathbb{R}^{N \times 1}$  and  $\mathbf{T} \in \mathbb{R}^{N \times 1}$  correspond to the phase shifts and time delays implemented by PSs and TTDs, respectively. Specifically,  $\Phi = [\psi_1, \dots, \psi_N]^T$  and  $\mathbf{T} = [t_1, \dots, t_N]^T$  where  $\psi_n \in [0, 2\pi]$  and  $t_n \in [0, t_{\max}]$  denote the phase shift and time delay in the  $n$ -th antenna element, respectively.

## III. SINGLE-SHOT POSITIONING VIA TRAINABLE NEAR FIELD RAINBOW BEAMFORMING

In this section, we introduce an end-to-end deep learning-based user localization scheme which aims to jointly optimize the beamforming design for sensing signal transmission and location algorithm for UE position estimation. We refer to it as Single-shot POSitioning via Trainable near-field rainbow beamforming scheme (SPOT). As illustrated in Fig. 2, the SPOT scheme comprises two key modules: (i) Beamformer: a complex-valued neural network (NN) that generates the downlink beamforming vector, and (ii) Estimator: a deep neural network (DNN) that reconstructs the user's position from the received feedback message. These modules are jointly optimized in an end-to-end fashion to minimize the root mean square error (RMSE) of both angular and range estimates.

### A. Module 1: Rainbow Beam Design

The generation of the downlink rainbow beam is modeled using a complex-valued NN module, which computes the complex-valued weights applied to each antenna element. The input to this NN module is the set of channel vectors  $\{\mathbf{h}_{k,m}\}$ . The trainable weights of the complex-NN layer are defined as  $\Theta_\Phi \in \mathbb{R}^{N \times 1}$  and  $\Theta_{\mathbf{T}} \in \mathbb{R}^{N \times 1}$ , representing the PS values and TTD values applied to each antenna element, respectively. To guarantee hardware feasibility, each parameter is projected into its physical range using a modulo operation:

$$\Phi = \text{mod}(\Theta_\Phi, 2\pi), \quad \mathbf{T} = \text{mod}(\Theta_{\mathbf{T}}, 1/f_{scs}). \quad (5)$$

Following the beamforming process, the received signal is obtained as described by (4). Instead of directly selecting the subcarrier with the maximum instantaneous power, we employ a temperature-scaled softmax function over the power values to obtain a probability distribution across subcarriers:

$$w_{k,m} = \frac{\exp(\alpha |y_{k,m}|^2)}{\sum_{m'=1}^M \exp(\alpha |y_{k,m'}|^2)}, \quad (6)$$

where the scaling factor  $\alpha > 0$  controls the sharpness of the probability distribution. The estimated soft subcarrier index is then computed as the weighted average of the subcarrier indices, rounded to the nearest integer:  $m_k^* = \text{round}\left(\sum_{m=1}^M w_{k,m} m\right)$ . The corresponding soft maximum power is then given by  $|y_{k,m_k^*}|^2$ . This approach ensures a smooth and differentiable selection of the dominant subcarrier.

### B. Module 2: User Localization

The position estimation process is implemented using a DNN, which takes the maximum received power  $|y_{k,m_k^*}|^2$  and the corresponding subcarrier index  $m_k^*$  as input. The input features are processed through three fully connected (FC) layers, where the output of each layer is denoted as  $\mathbf{v}_i$  for  $1 \leq i \leq L$ . To constrain the angle  $\hat{\phi}_k \in [-\pi/3, \pi/3]$  and ensure distance  $\hat{r}_k > 0$ , activation functions are applied:

$$\hat{\phi}_k = \frac{\pi}{3} \tanh(\mathbf{v}_{L,1}), \quad \hat{r}_k = \text{Softplus}(\mathbf{v}_{L,2}),$$

where  $\mathbf{v}_L = [\mathbf{v}_{L,1}, \mathbf{v}_{L,2}]$  is the final DNN output.

### C. Loss Function and Computational Complexity

The network is trained using a loss function defined as the RMSE of 2D localization:

$$\mathcal{L} = \sqrt{\frac{1}{K} \sum_{k=1}^K [(\hat{x}_k - x_k)^2 + (\hat{y}_k - y_k)^2]}, \quad (7)$$

where  $\hat{x}_k = \hat{r}_k \cos \hat{\phi}_k$  and  $\hat{y}_k = \hat{r}_k \sin \hat{\phi}_k$  denote the estimated Cartesian coordinates.

The proposed network's main computational cost lies in Module 2, a DNN with  $L$  FC layers. With  $N_0 = 2$  input neurons (power and subcarrier index),  $N_L = 2$  output neurons (angle and distance), and hidden layers  $N_1$  to  $N_{L-1}$ , its per-user complexity is  $\mathcal{O}\left(\sum_{\ell=0}^{L-1} N_\ell N_{\ell+1}\right)$ .

## IV. NUMERICAL RESULTS

Unless explicitly stated otherwise, the simulations are conducted using the parameters detailed in Table I. It is worth noting that the Rayleigh distance for our simulation setup is 348.35 meters. In our simulations,  $K$  users are assumed to be uniformly and randomly distributed within a spatial sector spanning  $[-60^\circ, 60^\circ]$  relative to the BS, with distances ranging from 5 to 300 meters. For the purpose of model development and evaluation, a dataset comprising 50 000 samples is generated for the training set, while 5000 independent samples are generated for the validation and test sets, respectively.

For comparison, we consider the following baselines:

- **CBS** [7]: Two stages of downlink transmissions include one beam for angle (CBS beam 1) and  $K$  user-specific beams for distance (CBS beam 2) estimation, respectively. Each user feeds back the peak-power subcarrier indices, enabling the BS to infer the position via the beam-split trajectory.
- **ConvNeXt** [8]: First runs CBS to get a coarse position estimate, then refines it with a ConvNeXt model that takes

TABLE I: Main notations and their typical values

Notation	Definition	Value
$f_c$	Central carrier frequency	28 GHz
$B$	Total bandwidth	380.16 MHz
$f_{\text{scs}}$	Subcarrier spacing	240 kHz
$N$	Number of antennas at BS	256
$M$	Number of subcarriers	1584
$\sigma^2$	Thermal noise power density	-174 dBm/Hz
$P_t$	Transmit power at BS	40 dBm
$N_1, N_2, N_3, N_4$	DNN parameters	64, 128, 64, 2

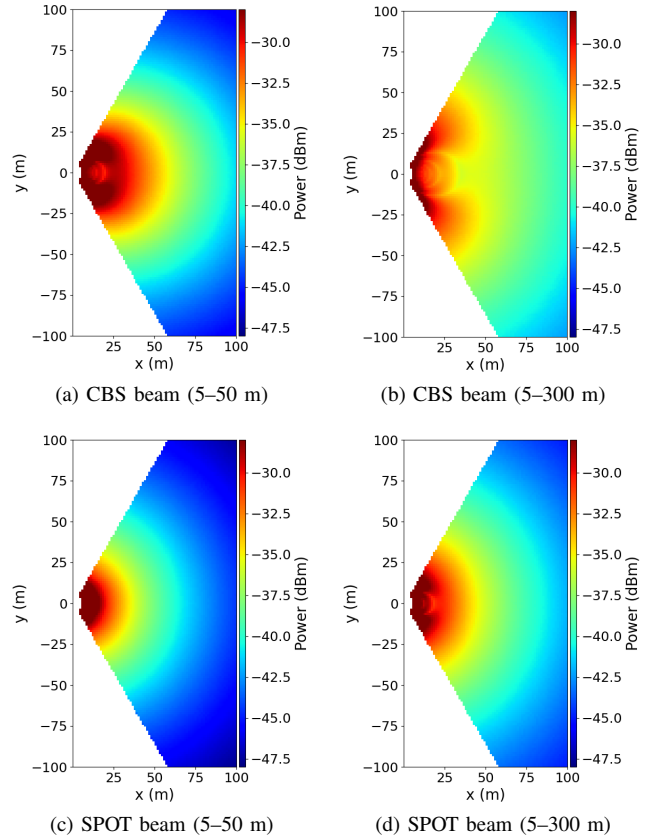


Fig. 3: Maximum received power of rainbow beam (dBm).

the two received power vectors and the coarse estimate as input.

- **Distance-dependent CBS** [9]: Uses distance-aware rainbow beams for joint angle–distance estimation within a single beam. Accuracy improves with more beams. Users estimate angles and distances locally and report to the BS.
- **RaiNet** [10]: We adapt the uplink-based RaiNet to our downlink scenario where the BS transmits CBS rainbow beams, and each user feeds back its received power vector across subcarriers. The BS employs the same convolutional and fully connected network architecture as in the original RaiNet to regress the user's position.

### A. Rainbow Beam Patterns

Fig. 3 illustrates the maximum received power of rainbow beams generated by the analytic CBS baseline and the

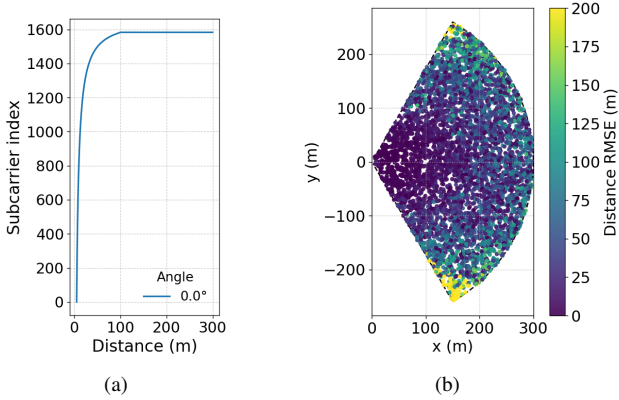


Fig. 4: Distance sensing performance of CBS approach. (a) Subcarrier index vs. distance mapping for a rainbow beam scanning from  $(0^\circ, 5 \text{ m})$  to  $(0^\circ, 300 \text{ m})$ . (b) Distance RMSE.

proposed SPOT design under two user-range priors: a near-range distribution (5–50 m) and a wide-range distribution (5–300 m). CBS exploits frequency-dependent focusing to trace a continuous spatial trajectory across OFDM subcarriers: the lowest-frequency subcarrier concentrates near a prescribed start point, the highest-frequency subcarrier focuses near a prescribed end point, and the intermediate subcarriers populate the path between them. The CBS beams in Fig. 3a and Fig. 3b are configured to span from  $(-60^\circ, 10 \text{ m})$  to  $(60^\circ, 10 \text{ m})$  and from  $(-60^\circ, 200 \text{ m})$  to  $(60^\circ, 200 \text{ m})$ , respectively. In contrast, the SPOT beam in Fig. 3c and Fig. 3d maintains an almost monotonic power–distance relationship over all angles, offering a stable foundation for power-based ranging. Moreover, SPOT dynamically adapts its power–distance profile to the user range: in near-range scenarios, pronounced power variations enable fine distance discrimination, whereas in wide-range scenarios, a deliberately smoother profile mitigates error accumulation over extended distances.

Fig. 4 examines the intrinsic relationship between subcarrier index and distance for CBS. As the user moves farther from the array, the beam of each subcarrier broadens owing to the weakening of near-field focusing, which flattens the index–distance curve in Fig. 4a. This compression of resolvable distance intervals degrades ranging precision at long ranges as shown in Fig. 4b. Consequently, CBS-based estimators that rely primarily on subcarrier indexing are well suited to compact, near-field coverage regions but scale poorly as the operating range expands.

### B. 2D RMSE under Different Maximum User Ranges

Fig. 5 reports the 2D localization RMSE versus the maximum user distance. The CBS, distance-dependent CBS, and ConvNeXt baselines all exhibit consistently higher errors than the proposed SPOT scheme, and their performance deteriorates more rapidly as the operating range expands. This behavior can be traced to two intrinsic limitations of these baselines. First, as shown in Fig. 4, the near-field focusing effect

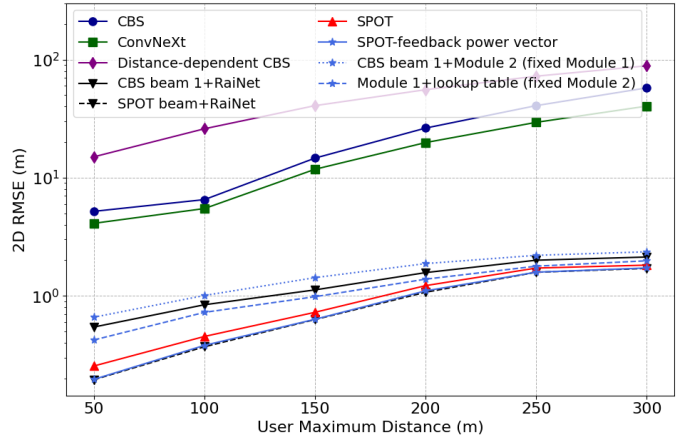


Fig. 5: 2D RMSE under different user maximum distances.

on which they depend weakens quickly with distance, so the subcarrier-index-to-distance mapping becomes coarse for far users, leading to a noticeable loss of ranging resolution. Second, these methods are vulnerable to error propagation from angle to range. Since they follow a two-stage procedure in which distance is inferred conditionally on the previously estimated angle, any angular inaccuracy in the first stage is directly amplified in the second-stage distance estimate.

Fig. 5 confirms that the original CBS-based RaiNet method in [10] (‘CBS beam 1 + RaiNet’) performs below the proposed SPOT scheme. Replacing the RaiNet downlink beam with the trained SPOT beam (‘SPOT beam + RaiNet’) reduces the RMSE by approximately 33.9% and outperforms the scalar SPOT scheme, which only feeds back the maximum power and its subcarrier index. Furthermore, when the SPOT input is changed to the full  $M$ -dimensional received power vector which matches the RaiNet input (‘SPOT-feedback power vector’), the estimation error is further reduced, achieving performance comparable to the SPOT beam-based RaiNet but with significantly lower model complexity.

An ablation study was conducted to validate the contributions of the two SPOT modules. When the beamforming module (Module 1) is fixed to the CBS beam while only the estimator (Module 2) is trained, the overall localization error is noticeably higher. Allowing the beamformer to be trainable lowers the average 2D RMSE by approximately 40.8% relative to this fixed baseline, underscoring the central role of beam optimization. Conversely, replacing the learned estimator (Module 2) with a non-learned simple distance lookup method increases the 2D RMSE by 31.24%. This lookup table is constructed by sampling power levels at various distances. This result validates the critical importance of the learned estimator for refining distance inference.

### C. 2D RMSE under Different Quantization Bit Lengths

Fig. 6 depicts the effect of power-feedback quantization bit length on the 2D RMSE of our SPOT scheme when users are distributed between 5 m and 300 m. The 2D RMSE of the quantized case ‘SPOT(Q)’ decreases exponentially as

TABLE II: Complexity and overheads comparison among five approaches.

Algorithm	FLOPs↓	Downlink Beams↓	Uplink Feedback Rounds per User↓	Overall Feedback Overhead ↓
CBS [7]	-	$1 + K$	2	$22K$ bits ( $2K$ indices)
Distance-dependent CBS [9]	-	10	1	$14K$ bits ( $K$ indices)
ConvNeXt [8]	4.98M	$1 + K$	2	$202752K$ bits ( $2K$ full signals)
RaiNet [10]	19.37M	1	1	$50688K$ bits ( $K$ signal powers)
SPOT	35.33k	1	1	$\leq 19K$ bits ( $K$ indices and $K$ quantized power values)

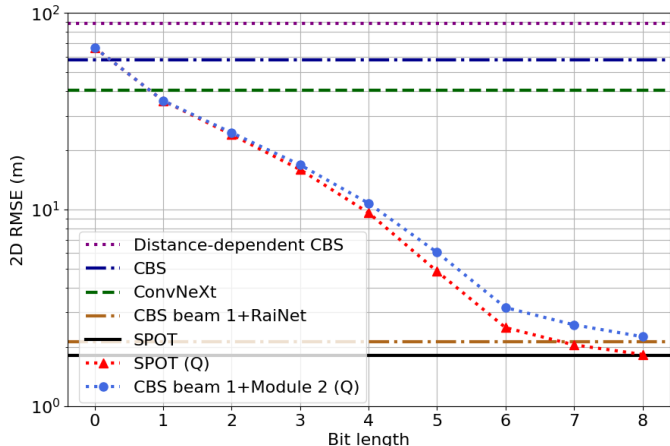


Fig. 6: 2D RMSE under different power quantization bit length.

the bit length increases from 1 to 5, and the performance nearly matches that of unquantized feedback at 8 bits. In addition, we evaluate a scheme with a fixed CBS beam and trained estimator (‘CBS beam 1 + Module 2 (Q)’). Results show that the joint training approach SPOT(Q) consistently achieves lower RMSE, with the performance gap widening as bit length increases. Specifically, joint training reduces the RMSE by 21.64% relative to the fixed-beam strategy at 8 bits quantization.

#### D. Overhead, Complexity, and Accuracy Comparison

Table II compares the overheads of SPOT and baseline algorithms. Both CBS and distance-dependent CBS incur minimal complexity, as they directly infer user location from pre-computed beam-splitting trajectories. In contrast, ConvNeXt refines a coarse estimate using a convolutional network that processes the full received-signal vector, greatly increasing computational and feedback costs. Moreover, CBS and ConvNeXt require two downlink transmissions with separate feedback for angle and distance estimation. For distance-dependent CBS, the base station sequentially transmits 10 distance-aware rainbow beams to sweep the entire angular-range plane, and the user reports back the subcarrier index corresponding to the strongest received power observed across all rounds. RaiNet requires only a single downlink transmission but incurs a high uplink cost due to the feedback of the full received-power vector and a larger network complexity of 19.37 M FLOPs. In contrast, SPOT attains the best trade-off between accuracy and efficiency, requiring merely 35.33k FLOPs with one downlink transmission and a single uplink message containing only two scalar values.

## V. CONCLUSION

In this paper, we proposed a novel end-to-end deep learning scheme for wideband ISAC systems employing PTAs. The core innovation lies in modeling PS and TTDs coefficients as learnable parameters within the network, enabling joint optimization of rainbow beam generation and user position estimation. Using only a single downlink transmission and compact uplink feedback containing the quantized maximum received power and its subcarrier index, the proposed method efficiently recovers both angle and distance, greatly reducing signaling overhead. Extensive simulations across a wide range of user distances demonstrate that our scheme attains lower localization RMSE with minimal cost. The performance advantage becomes more pronounced in far-field scenarios, demonstrating strong robustness across diverse propagation conditions.

## REFERENCES

- [1] N. González-Prelcic, D. Tagliaferri, M. F. Keskin, H. Wymeersch, and L. Song, “Six Integration Avenues for ISAC in 6G and Beyond,” *IEEE Vehicular Technology Magazine*, vol. 20, no. 1, pp. 18–39, Mar. 2025.
- [2] V. V. Ratnam, J. Mo, A. Alammouri, B. L. Ng, J. Zhang, and A. F. Molisch, “Joint phase-time arrays: A paradigm for frequency-dependent analog beamforming in 6G,” *IEEE Access*, vol. 10, pp. 73 364–73 377, 2022.
- [3] Y. Cai, M. Tao, and S. Sun, “Frequency-Dependent Beamforming for Hybrid Near-Far Field Communications Through Joint Phase-Time Arrays,” in *2025 IEEE Wireless Communications and Networking Conference (WCNC)*, 2025, pp. 1–6.
- [4] Y. Cai, M. Tao, J. Mo, and S. Sun, “Hybrid Near/Far-Field Frequency-Dependent Beamforming via Joint Phase-Time Arrays,” *arXiv preprint arXiv:2501.15207*, 2025.
- [5] J. Mo, A. Alammouri, S. Dong, Y. Nam, W.-S. Choi, G. Xu, and J. C. Zhang, “Beamforming with Joint Phase and Time Array: System Design, Prototyping and Performance,” in *2024 58th Asilomar Conference on Signals, Systems, and Computers*. IEEE, 2024, pp. 875–881.
- [6] F. Gao, L. Xu, and S. Ma, “Integrated sensing and communications with joint beam-squint and beam-split for mmWave/THz massive MIMO,” *IEEE Transactions on Communications*, vol. 71, no. 5, pp. 2963–2976, 2023.
- [7] H. Luo, F. Gao, W. Yuan, and S. Zhang, “Beam Squint Assisted User Localization in Near-Field Integrated Sensing and Communications Systems,” *IEEE Transactions on Wireless Communications*, vol. 23, no. 5, pp. 4504–4517, 2024.
- [8] H. Lei, J. Zhang, H. Xiao, D. W. K. Ng, and B. Ai, “Deep Learning-Based Near-Field User Localization With Beam Squint in Wideband XL-MIMO Systems,” *IEEE Transactions on Wireless Communications*, vol. 24, no. 2, pp. 1568–1583, 2025.
- [9] T. Zheng, M. Cui, Z. Wu, and L. Dai, “Near-Field Wideband Beam Training Based on Distance-Dependent Beam Split,” *IEEE Transactions on Wireless Communications*, vol. 24, no. 2, pp. 1278–1292, 2025.
- [10] R. Klus, J. Talvitie, I. Pehlivan, M. C. Ilter, L. Klus, D. Cabric, and M. Valkama, “Deep Learning Based Near-Field Positioning in True-Time-Delay Array Systems,” in *2025 IEEE 26th International Workshop on Signal Processing and Artificial Intelligence for Wireless Communications (SPAWC)*, 2025, pp. 1–5.